LIGHTNING INDUCED CURRENTS IN AIRCRAFT WIRING USING LOW LEVEL INJECTION TECHNIQUES

E G Stevens
ERA Technology Ltd, UK

D T Jordan
Royal Aerospace Establishment, UK

ABSTRACT

Various techniques have been investigated to predict the transient current induced into aircraft wiring bundles as a result of an aircraft lightning strike. A series of practical aircraft measurements have been carried out together with a theoretical analysis using computer modelling. These tests have been applied to various aircraft and also to specially constructed cylinders installed within coaxial return conductor systems.

Low level swept frequency cw (carrier wave), low level transient and high level transient injection tests have been applied to the aircraft and cylinders. Measurements have been carried out to determine the transfer function between the aircraft drive current and the resulting skin currents and currents induced on the internal wiring. The full threat lightning induced transient currents have been extrapolated from the low level data using Fourier transform techniques.

The aircraft and cylinders used in these investigations were constructed from both metallic and CFC (carbon fibre composite) materials. The results demonstrate the pulse "stretching" phenomenon which occurs for CFC materials due to the diffusion of the lightning current through carbon fibre materials. TLM (transmission line matrix) modelling techniques have been used to compare the theoretical currents and the measured values.

INTRODUCTION

This paper provides a summary of various ongoing lightning simulation techniques which have been investigated during trials by ERA and RAE to evaluate the indirect effects of lightning strikes to aircraft using low level cw and transient injection techniques.

The investigations have primarily been concerned with measurements of currents induced into the aircraft wiring harnesses as a consequence of low level injection into an aircraft fuselage. To investigate these effects various test rigs were erected around ground based aircraft and specially constructed test cylinders including:

* aluminium cylinder
* carbon fibre cylinder
* modern non-metallic helicopter
* modern carbon fibre aircraft
* modern metallic aircraft

Each of the test subjects were fitted with specially designed return conductor systems which were derived from the results of computer modelling such as "INDCAL", and using the experience and engineering judgement of the engineers involved.

CYLINDER MEASUREMENTS

Two cylindrical tubes were constructed and installed within coaxial return conductor systems to investigate the effects of lightning coupling to a wire within the cylinder. One of the cylinders was constructed from aluminium and the other from CFC materials.

The primary objectives of the tests were to compare the results obtained using transient injection techniques with the cw injection techniques, using various termination load resistance values.

Cylinder Configuration

The cylinders were approximately 1.5 m long, 0.5 m in diameter and were constructed using material of approximately 2 mm in thickness. The ends of the cylinders were fitted with 60 degree tapered conical extensions made from eight copper bars (1/2" x 1/16") and were attached using a circular copper fixing band. Electrical contact to the CFC cylinder was achieved by electroless plating the ends of the cylinder using a solution of a copper salt.

In addition each cylinder was fitted with a coaxial return conductor system approximately 2.4 m long and 1.15 m diameter, made from eight copper conductors (1/2" x 1/16"). The return conductor system was tapered at each end to maintain a constant characteristic impedance of approximately 50 Ω. The cylinders were each fitted with internal test wires which could be terminated with various loads via "N" type connectors. The design of the cylinders and return conductor system is shown in Figs.1 and 2.

Cylinder Tests

The transient injection tests were carried out at low level using a digital waveform generator which produced a double exponential signal with a peak amplitude of approximately 14 A, a risetime of 13 μs (time to peak) and a half amplitude duration of 102 μs.

Transient injection was also carried out at medium level using an RAE transient generator which produced a double exponential signal with a peak amplitude of approximately 1100 A, a risetime of 16 μs (time to peak) and a half amplitude duration of 58 μs.

The swept frequency cw injection tests were carried out over the frequency range 10 Hz to 100 MHz using a network analyser together with a selection of amplifiers. The magnitude and phase angle of the current induced on the test wire was normalised to the cylinder drive current to obtain the transfer function. The induced current measurements were made using current probes.

Cylinder Results

The cw transfer function measurements have been normalised to the transient drive waveforms using Fourier transform techniques to compare the results obtained using the two methods.

Comparing the results from the transient injection tests carried out in the time domain with the cw injection tests carried out in the frequency domain shows that similar results are obtained.

Figs.3 and 4 show typical graphs which compare the wire current results obtained by the two test techniques for the 1100 A transient using the aluminium cylinder and the CFC cylinder terminated with 50 Ω. The X-axis time scale is logarithmic to allow the full transient waveform to be observed.

For the aluminium cylinder the initial wire transient shape approximates towards the differential of the driving transient followed by an overshoot and a "long tail". For the CFC cylinder the wire current is a similar shape to the drive current waveform.

The cw results have also been extrapolated to the "Component A and H" lightning waveforms as specified in the "Yellow" book Ref.[1] and in the "Orange" book Ref.[2], to compare the currents. The highest currents are induced with the CFC cylinder with short circuit loads on the both the wire and the cylinder.

For the "Component A" threat (Fig. 5) the peak wire current for the CFC cylinder is 49 kA at 61 μs and for the aluminium cylinder the wire peak current is 2.3 kA at 7.8 μs.

For the "Component H" threat (Fig 6) the peak wire current for the CFC cylinder is 450 A at 10 μs and for the aluminium cylinder the wire peak current is 140 A at 0.3 μs. The transient on the wire in the CFC cylinder is considerably "stretched" in time compared the "Component A and H" threat waveforms which peak at 6.4 μs and 0.25 μs respectively.

Cylinder TLM Modelling

The cylinder and return conductor system have also been modelled using 3D (three dimensional) TLM modelling to predict the current induced on the cylinder wire, Ref [3]. The 3D model uses a regular mesh size of 0.05 m which represents a mesh cut-off frequency of 600 MHz (assuming 10 cells per wavelength).

As a consequence of the inherent symmetry in the return conductor system a parallel processing approach was used to enable the Sun3 to be used with transputers. The eight return conductors have been reduced to four to enable the four transputers to be implemented in the processing.

The induced wire current has been modelled at the same positions where the practical measurements were carried out. The impulse response has been filtered down to 100 MHz and convolved with a double exponential threat waveform with a peak amplitude of 1 A, a risetime of 1 μs (time to peak) and a half amplitude duration of 20 μs.

The predicted transient current is shown in Figs.7 and 8 respectively for aluminium and CFC cylinders terminated with a 50 Ω load. The currents in the wire, the current in the cylinder and the current in the return conductor system are shown. The maximum time duration shown on the graph is only 16 μs, however the wire current for the CFC cylinder (shown as No 2 on the graph in Fig.8), has not yet reached its peak value, indicating a considerable time elongation of the transient.

The computer processing time required to calculate the currents is considerable and the work is currently being updated to include longer time durations for the predicted data.

HELICOPTER MEASUREMENTS

As part of the AFARP 17 (Anglo-French aeronautical research programme) a series of lightning simulation tests have been applied to an Aerospatiale Ecureuil helicopter, Refs [4] and [5]. The tests were carried out at CEAT (Centre d'Essais Aeronautique de Toulouse) in France during 1989/90 by teams from RAE (Royal Aerospace Establishment) Farnborough UK, ONERA (Office National d'Etudes et de Recherches Aerospatiales) Meudon France, and CEAT.

The helicopter was installed within a coaxial return conductor system consisting of nine flexible conductors to form a coaxial line from the nose to the tail of the aircraft to simulate a nose to tail strike. A number of instrumentation wires were installed within the aircraft for the measurement of induced currents.

The return conductor system was terminated at the tail using various loads including the characteristic impedance of the transmission line (approximately 50 Ω) and also using an open circuit and also short circuit loads.

Helicopter Tests

Various tests were applied by each of the trials teams and included:

* low level swept frequency carrier wave injection (by RAE)
* low and medium level transient injection (by CEAT)
* high voltage transient injection (by ONERA)

The low level transient injection tests were carried out using a reduced level waveform similar to lightning "Component H" (H/10), with a peak amplitude of approximately 1 kA, a risetime of 100 ns and a duration of 4 μs.

Transient injection was also carried out at medium level using a waveform similar to in shape to a lightning "Component D" (D/20) waveform with a peak amplitude of approximately 6 kA, a risetime of 3 μs and a duration of 30 μs. At higher levels the peak amplitude was increased to 50 kA (D/2) with a risetime of 3 μs and a reduced duration of 15 μs.

The swept frequency cw injection tests were carried out over the frequency range 1 kHz to 100 MHz using a network analyser together with a selection of amplifiers. The magnitude and phase angle of the current induced on the measurement wiring bundle was normalised to the aircraft drive current to obtain the transfer function. The induced current measurements were made using current injection and current measuring probes.

Helicopter Results

A comparison has been made between results of the wire currents predicted from the cw measurements extrapolated to the aircraft threat test transient and the wire currents measured during the transient injection tests.

There is a very good agreement between the transient shapes obtained using the two test techniques although amplitude of the cw predictions is higher than the transient measurements. Typical graphs for different wires are shown in Figs.9 and 10 for the "Component D" waveform and in Figs.11 and 12 for the "Component H" waveform.

CFC AIRCRAFT MEASUREMENTS

A series of lightning simulation tests have been applied to a modern jet aircraft constructed from CFC materials to investigate coupling phenomena.

High level transient injection and low level swept frequency cw injection transfer function tests were applied to investigate the degree of coupling between the airframe and the aircraft wiring bundles. The aircraft was installed on aircraft jacks within a return conductor system configured for a nose to wing tip lightning strike.

CFC Aircraft Tests

The cw transfer function measurements were made between the drive current into the aircraft and the induced current on the aircraft wiring bundles and extrapolated to the test transient used during the aircraft. Measurements were made with the aircraft electrically inert and also electrically powered from a ground power unit to investigate any differences.

The transient injection was carried out at using a Culham LTT transient generator which produced a double exponential signal with a variable peak amplitude of up to approximately 40 kA, with a risetime of approximately 2.5 μs (time to peak) and a half amplitude duration of 14 μs.

CFC Aircraft Results

A comparison has been made between results of the wire currents predicted from the cw measurements extrapolated to the aircraft threat test transient and the wire currents measured during the transient injection tests. There was no significant difference in the swept frequency cw transfer function measured with the aircraft powered and un-powered.

There is a good agreement between the cw and transient test techniques and the results obtained for two typical wiring bundles are shown in Figs.13 and 14.

The cw results for a typical wiring bundle have been normalised to the "Component A" and "Component H" waveforms in Figs.15 and 16. For the "Component A" waveform the peak current occurs at approximately 100 μs with a level of over 400 A. Also for the "Component H" waveform it can be seen that considerable elongation has occured.

METALLIC AIRCRAFT MEASUREMENTS

A series of swept frequency cw skin current measurements have been applied to a modern metallic aircraft at the RAE (Royal Aerospace Establishment) Farnborough UK. The aircraft was installed within a return conductor system to simulate a lightning strike entering at the aircraft nose and exiting at the tail. The return conductor system consisted of twelve copper tubular conductors to form a coaxial line, Refs[6], [7] and [8].

Metallic Aircraft Tests

Swept frequency cw skin current measurements of transfer function were made at various locations over the aircraft fuselage. The reference skin current was initially measured at the 1 m circumference position on the nose injection point on the aircraft. The transfer function was measured at various positions along the fuselage and out onto the wings of the aircraft as shown pictorially in Fig.17 (return conductor system omitted for clarity).

The return conductor system was terminated in turn by its characteristic impedance, by a short circuit and also by an open circuit. The measurements covered the frequency range 100 Hz to 100 MHz and were carried out using direct injection techniques into the aircraft nose and measurement of the transfer function using a skin current probe and a network analyser.

Metallic Aircraft Results

The results are shown as the magnitude and phase angle of the skin current with respect to the nose injected skin current. In general the skin current was reasonably uniform for frequencies below approximately 3 MHz (resonance of return conductor system) and varied approximately as expected with the size of the surface circumference of the aircraft fuselage. At higher frequencies the skin current varied by up to +/- 30 dB at some of the resonant frequencies. Typical results are shown in the following section on modelling.

Metallic Aircraft TLM Modelling

The aircraft and return conductor system have been modelled using 2D (two dimensional) and 3D (three dimensional) TLM (transmission line matrix) modelling to predict the cw response of the airframe Refs [9] and [10]. The 3D model uses a mesh size of 0.21 m (143 MHz mesh cut-off frequency) and represents the twelve return conductors as eight flat plates. The number of return conductors was reduced to allow a sufficient number of TLM nodes between the return conductors to obtain the correct magnetic field distribution.

The airframe skin current has been modelled at the same positions where the practical measurements of skin current were carried out. Both the magnitude and phase angle of the skin current have been modelled and compare well with the measured values at all locations. Figs.18 and 19 compare the magnitude and phase angle of the measured skin current transfer function with the modelled values.

It is hoped that these modelling techniques will be extended for future work to assist with the prediction of lightning transient currents on aircraft equipment and wiring bundles.

CONCLUSIONS

Various swept frequency cw and transient injection techniques have been examined and compared to investigate the indirect effects of an aircraft lightning strike and the coupling to aircraft equipment and wiring bundles. There is a good correlation between the results obtained using these two techniques.

TLM modelling techniques have been used to predict the skin current distribution on aircraft and the currents induced onto wires inside cylinders. A good correlation has been achieved between the modelled values and practical measurements.

ACKNOWLEDGEMENT

Acknowledgement is given to Messers S I Holland of ERA Technology Ltd and S J Holden of A&AEE Boscombe Down for carrying out the practical measurements to assist with the preparation of this paper.

REFERENCES

1 Yellow Book, "Test waveforms and techniques for assessing the effects of lightning induced transients". SAE committee report AE4L-81-2, 15th December 1981

2 Orange Book, "Protection of aircraft electrical/electronic systems against the indirect effects of lightning", Recommended draft advisory circular. SAE AE4L-87-3 Committee Report, 4th February 1987.

3 Mallik A., "Convert TLM code to OCCAM and produce a 3D model of a CFC fuselage", KCC report 201/WS3, MOD contract AWL12C/2694, Kimberley Communication Consultants Ltd, Nottingham UK, July 1990.

4 Emanuely J.L, Daviose C., "Lightning simulations on a helicopter test-bed: pulse injection test results (Part 1: raw measurements)", Anglo-French research programme (AFARP) No 17, E88/681500 part 1, reference 001230, Centre D'essais Aeronautique de Toulouse (CEAT), France, 4 February 1991.

5 Emanuely J.L, Daviose C., "Lightning simulations on an helicopter test-bed. Part 2: Synthesis", Anglo-French research programme (AFARP) No 17, E88/681500 part 2, reference 002276 8 March 1991, Centre D'essais Aeronautique de Toulouse (CEAT), France.

6 Stevens E.G., "Assessment and application of whole aircraft lightning test techniques", ERA report 89-0312, ERA Technology Ltd, Leatherhead, Surrey, April 1990.

7 Stevens E.G., Jordan D.T., Holden S.J., "Whole aircraft lightning indirect effects evaluation using low level injection techniques", International conference on lightning and static electricity, University of Bath, 26 to 28 September 1989.

8 Stevens E.G., "Lightning test techniques using low level injection for indirect effects evaluation", draft ERA Report 90-0155, ERA Technology Ltd, Leatherhead UK.

9 Armour T., Mallik A., "Lightning interaction with aircraft". KCC Report No 146/5, Contract A85C/2420, Kimberley Communications Consultants Ltd, Nottingham, May 1987

10 Johns D.P., "TLM predictions of the response of a Jaguar aircraft in a lightning rig", KCC report 182/WS2, MOD contract AWL 12C/2612, Kimberley Communications Consultants Ltd, Nottingham, UK, 21 January 1991.

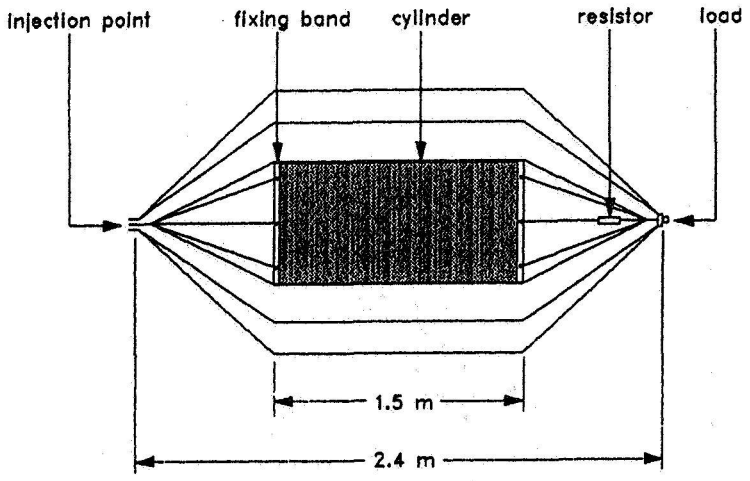

Fig.1 Cylinder and Return Conductor System (Side view)

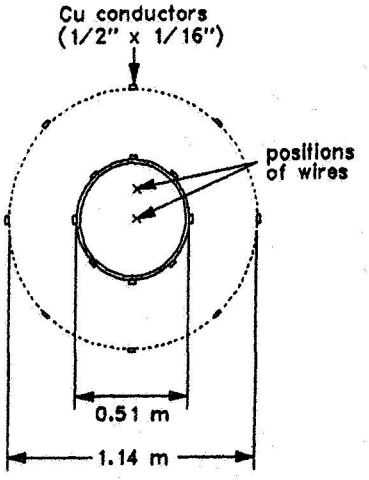

Fig.2 Cylinder and Return Conductor System (End view)

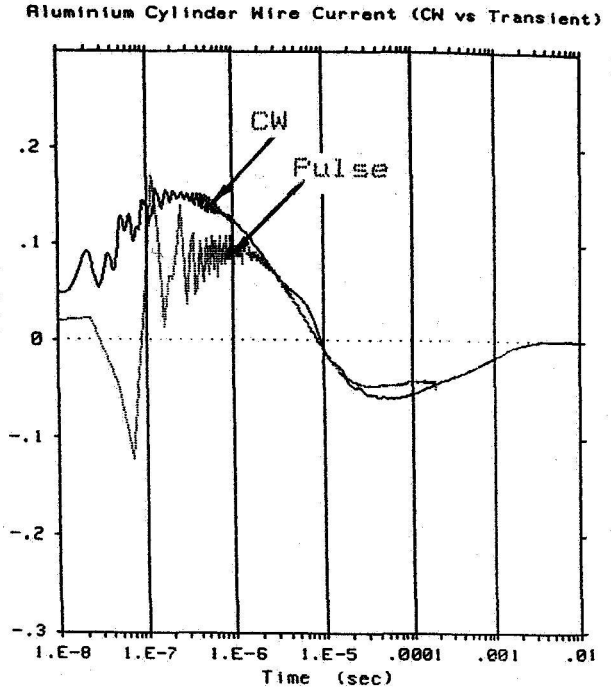

Fig.3 Aluminium Cylinder Wire Current (CW versus Pulse)

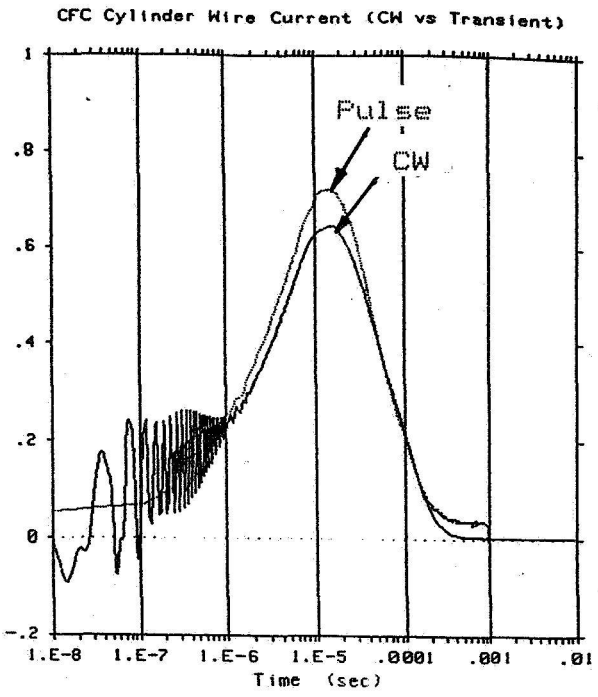

Fig.4 CFC Cylinder Wire Current (CW versus Pulse)

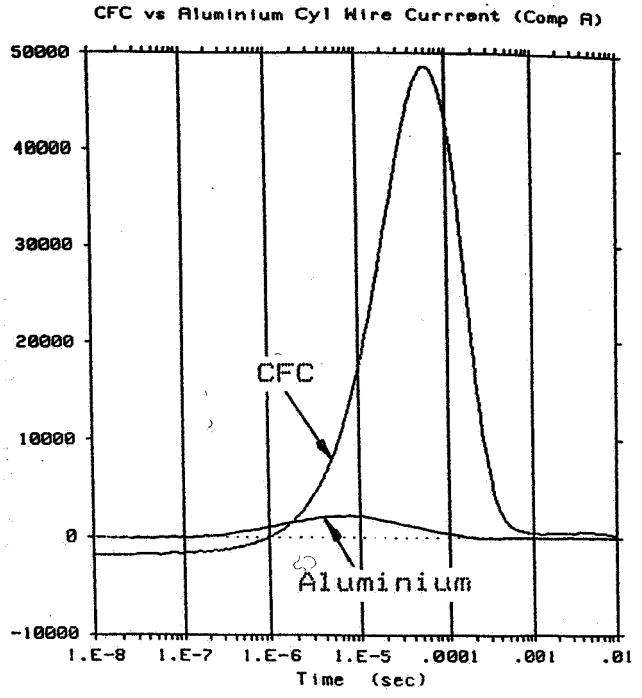

Fig.5 Aluminium versus CFC Cylinder Short Circuit Wire Current (Component A)

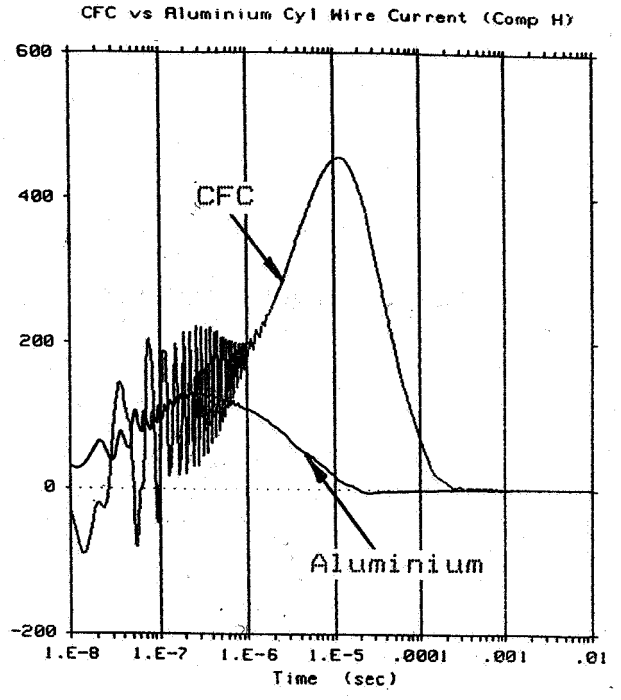

Fig.6 Aluminium versus CFC Cylinder Short Circuit Wire Current (Component H)

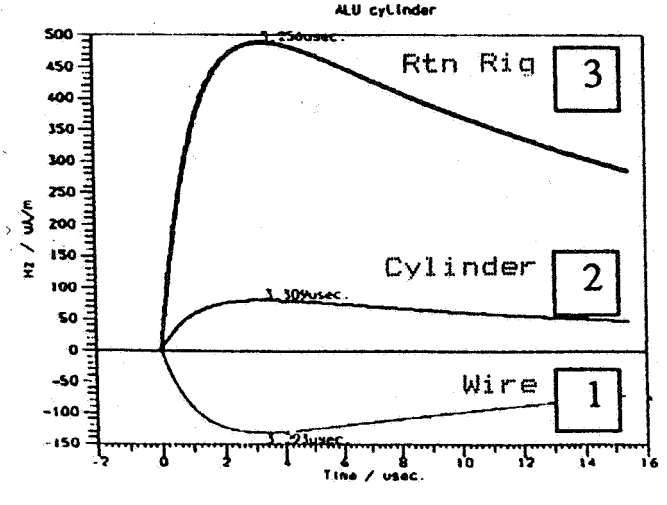

Fig.7 TLM Modelled Cylinder Currents (Aluminium Cylinder)

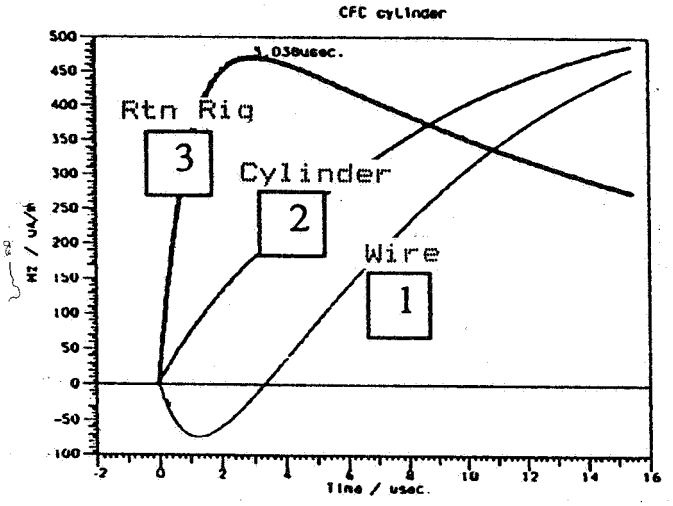

Fig.8 TLM Modelled Cylinder Currents (CFC Cylinder)

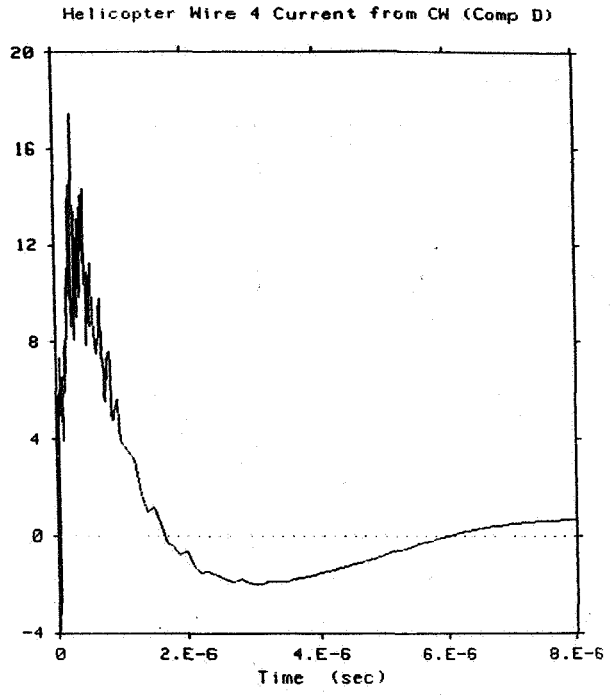

Fig.9 Helicopter CW Predicted Wire Transient (Wire 4, Component D)

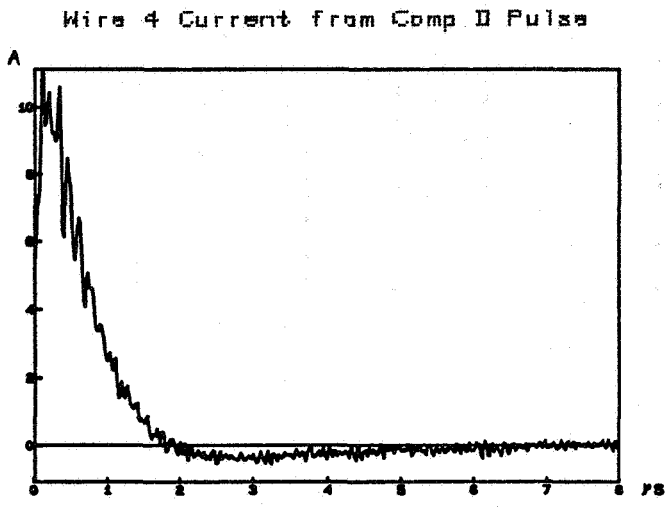

Fig.10 Helicopter Transient Wire Measurement (Wire 4, Component D)

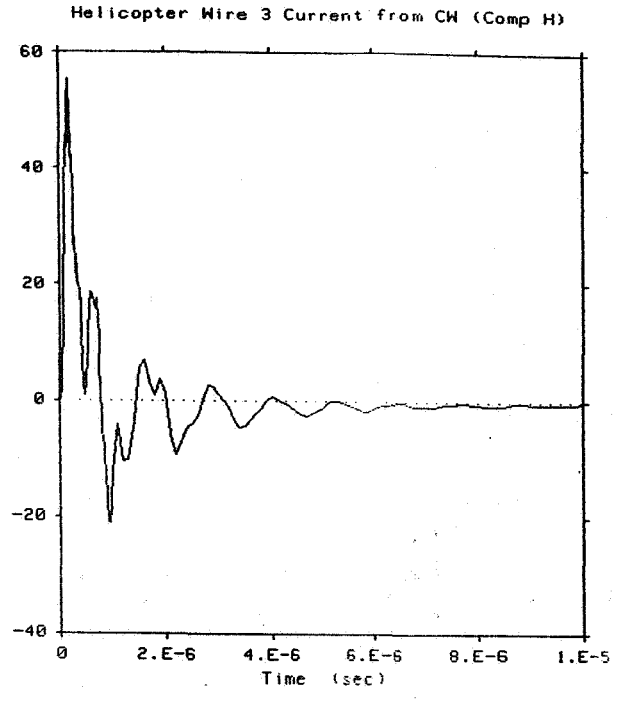

Fig.11 Helicopter CW Predicted Wire Transient (Wire 3, Component H)

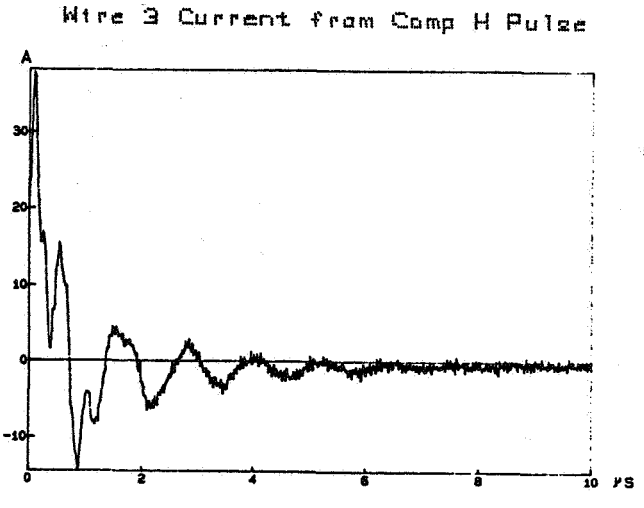

Fig.12 Helicopter CW Predicted Wire Transient (Wire 3, Component H)

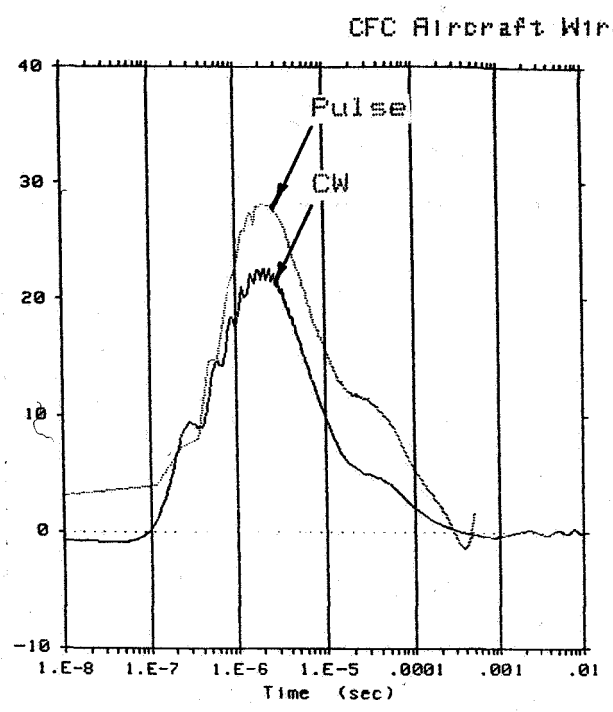

Fig.13 CFC Aircraft Typical Wiring Transient (CW versus Pulse)

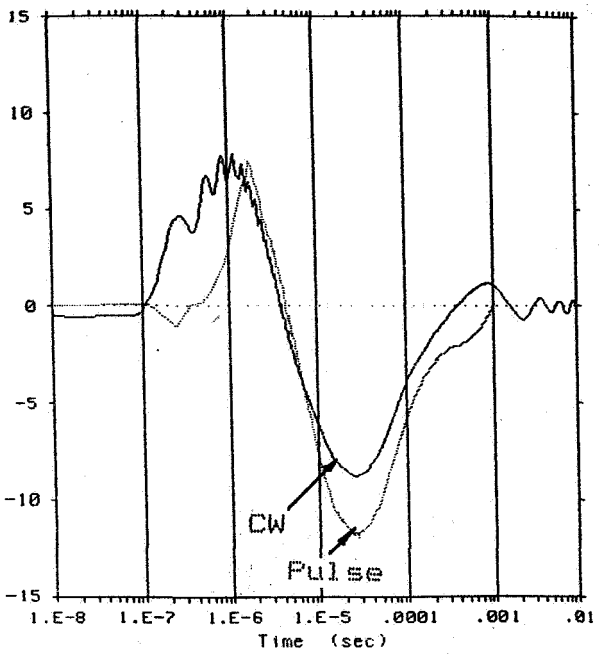

Fig.14 CFC Aircraft Typical Wiring Transient (CW versus Pulse)

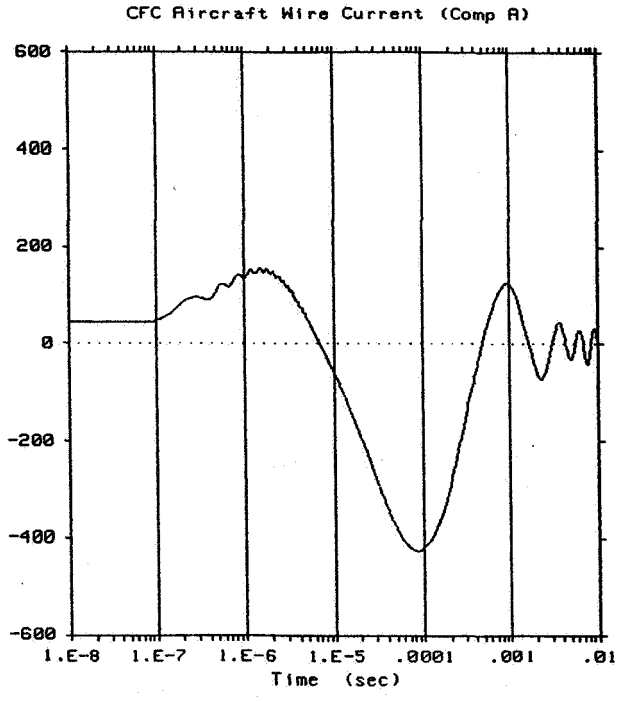

Fig.15 CFC Aircraft Typical CW Predicted Wiring Transient (Component A)

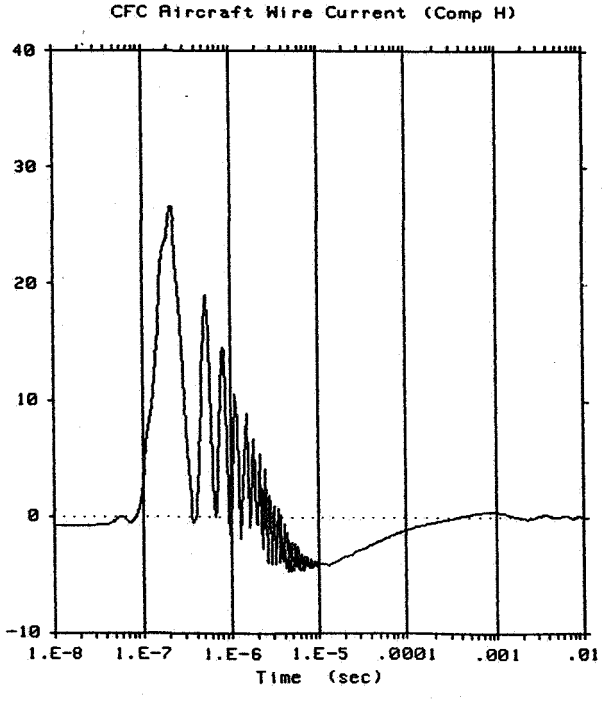

Fig.16 CFC Aircraft Typical CW Predicted Wiring Transient (Component H)

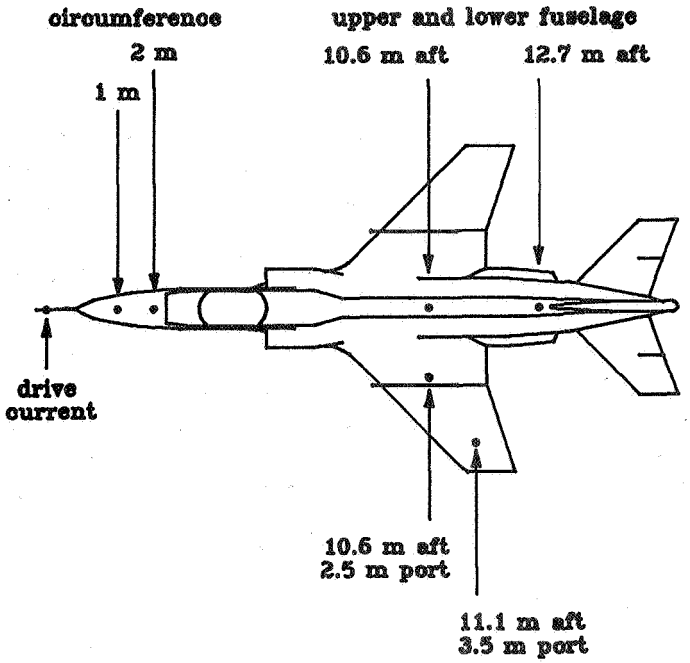

Fig.17 Metallic Aircraft Skin Current Measurement Locations

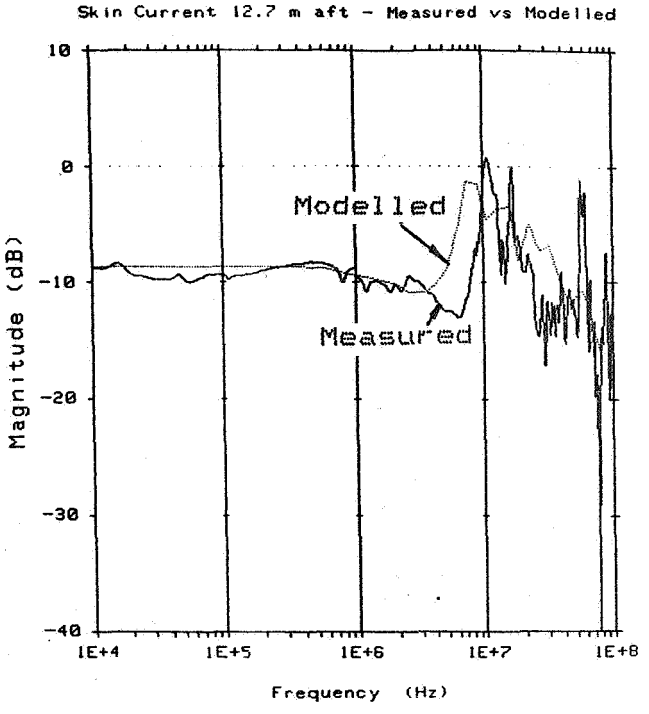

Fig.18 Metallic Aircraft Skin Current Magnitude Transfer Function (Modelled versus Measured)

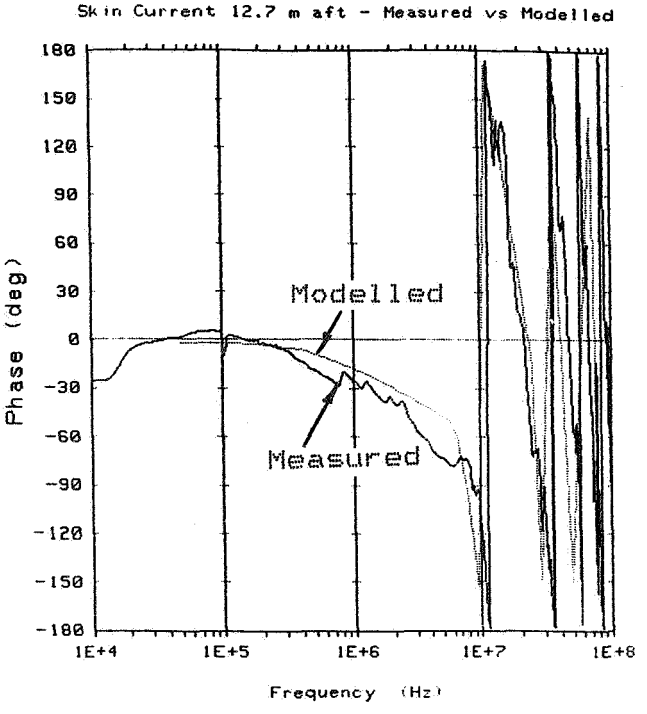

Fig.19 Metallic Aircraft Skin Current Phase Transfer Function (Modelled versus Measured)